

Submitted to

Dr. Alejandro Allievi PhD, PEng

alejandro.allievi@concordia.ca

Submitted by

Group# 18

Satnam Singh Bhullar

ID: 40083607

Masters of Engineering, Mechanical

S_BHUL@encs.concordia.ca

Noel Peter D'souza

ID: 40054636

Masters of Engineering, Aerospace

Faizan Ahmed

Masters of Engineering, Mechanical

ID: 40091062

Hussam Ktaily

ID: 40089897

Masters of Engineering, Mechanical

PROJECT REPORT ON

Lid Driven Square Cavity Flow at Reynolds number 100 and Flow over Circular Cylinder at Re 3200 and 10000: ANSYS Computational Fluid Dynamics, Fluent.

Date Submitted

Hard Copy 3 December 2018

Soft Copy 3 December 2018

ABSTRACT

A general setup of simulation is modeled to compute the solution of unsteady, incompressible Navier-Stokes equations for laminar flow. Results for this significant engineering subject are reproduced using ANSYS Fluent; a computational fluid dynamics (CFD) software, in comparison with algorithmic approach of finite element modified method of characteristics (FEMMC). This multigrid method tends to produce results in close approximation to the algorithmic approach with high mesh refinements in triangular and quad computations. Higher convergence rates can be achieved with greater discretization of the problem to study at more infinitesimal points which takes more time due to increased number of iterations. Numerical results of the computational analysis are illustrated for Navier-Stokes solution of:

- I. Lid-driven square cavity flow at Reynolds numbers as high as $Re=3200$ & $Re=10,000$
- II. Flow around a circular cylinder at low Reynolds number of $Re=100$

Key Words: Multigrid method, ANSYS Fluent, Viscous incompressible Navier Stokes equations, lid-driven cavity, Vortices, circular cylinder, Vortex shedding

1. INTRODUCTION

Developing an efficient finite element method for the Stokes and Navier-Stokes equations is a significant element in incompressible flow simulation [1]. Over the decades, solutions to stationary Navier-Stokes equations with some strong individuality condition are conferred by various authors [2-5], adopting some efficient reiterative strategies. The modified method of characteristics (MMC) was first presented by Benque' et al. [6], Douglas and Russell [7], and Pironneau [8] proceeded with further resolution for the Navier-Stokes equations. Additional enhancements have been conferred by Dawson et al. [9], and Buscaglia and Dari [10] demonstrated the numerical tests.

The methodology employed by [6,7,8], involves L2-projection on the finite element space to interpret the position of the particles of fluid at the foot of the characteristic, that leads to the assessment of integrals, which have been acknowledged by [7,8] and some others, to be the crucial step of this technique. In lieu of this approach, a search-locate algorithm have been adapted by Allievi and Bermejo [11]. In another paper by Allievi et al. [12], they achieved the numerical results of the common yet complex Navier-Stokes problems of lid driven cavity flow and flow around a circular cylinder by applying the method of preconditioned conjugate gradient, conferred by Cahouet and Chabard [13] and by Glowinski and collaborators [14,15].

Over the decades, all these comprehensive efforts along with advancement in computer technology have contributed in successfully analyzing vast fluid flow problems, despite involving more complications. Since, the solution to Navier-Stokes problems comprises abundant iterations with discretization of equations to be applied at numerous computational points, researchers have adapted various new techniques to attain higher convergence rates and found them more effective, as admired by Ghia et al. [16]. Among them are the unstructured grids, multigrid, operator splitting, domain decomposition and mesh adaptation techniques. Continuous efforts have been made since long, to enhance the solutions of incompressible flows and other problems by comparing such techniques, witnessed by DFG Priority Research Program [17].

In this work, while keeping in mind some important factors such as Reynolds number, mesh size and total points of computation that have a direct impact on the convergence rate, we have employed ANSYS Fluent (a CFD solver based on Multigrid method [18]), to compute the numerical results for lid driven square cavity flow and flow around a circular cylinder. The two-dimensional lid-driven square cavity problem holds significant importance in the scientific research due to its geometric simplicity, exhibiting most of the fluid mechanical phenomenon for viscous incompressible flows. Hence, it has been employed repeatedly to verify the accuracy and efficiency of various numerical methods. Simulations have been performed at Reynolds number 3200 and 10,000 to observe the streamline contours displaying the separation phenomena and vortices developed at the three corners. The second problem of flow behind a circular cylinder holds high practical significance in engineering as well. At low Reynolds number of $Re=100$, flow around the cylinder have been observed at equal time intervals. Though, all the conditions are kept steady, vortex shedding occurs after the formation of two eddies at the wake of cylinder, which grow bigger with time to cause unsteadiness. Accordingly, drag and lift properties have been observed to change with

time respectively. All the flow variables and boundary conditions are kept in agreement with the work done by Allievi et al. [12], to obtain the numerical results in close proximity for a good characteristic comparison.

The report is organized as follows. In the next content, we demonstrate the methodology employed on ANSYS Fluent and the basic algorithm behind the software to solve the Navier-Stokes equations for both problems. We then present our numerical results for each problem in comparison with the results obtained in [12] with all the constants and conditions defined. Finally, we make a brief conclusion at the end of the report.

2. METHODOLOGY

Initial Setup of CFD Solver

FLUENT solves the equations of Conservation of Mass and Momentum for all flows except flows involving transfer or compressibility. In such cases, energy conservation is solved additionally. When a flow is turbulent, additional transport equations are solved [19]. Even though the Navier Stokes equations are recognized as the conceptual model for fluid flows they contain 3 major approximations which are [20]:

- (a) Continuum hypothesis
- (b) Form of the diffusive fluxes
- (c) Equation of state

They also contain some difficulties such as non-linearity, coupling and the role of pressure. Incompressible flows use simpler conceptual models and use many additional assumptions.

Conservation of Mass (Continuity in 2 Dimensions)

$$\frac{\partial u}{\partial x} + \frac{\partial v}{\partial y} = 0 \quad \text{and}$$

$$\frac{\partial u}{\partial t} = -\frac{\partial u^2}{\partial x} - \frac{\partial uv}{\partial y} - \frac{1}{\rho} \frac{\partial p}{\partial x} + \frac{1}{Re} \left(\frac{\partial^2 u}{\partial x^2} + \frac{\partial^2 u}{\partial y^2} \right)$$

$$\frac{\partial v}{\partial t} = -\frac{\partial uv}{\partial x} - \frac{\partial v^2}{\partial y} - \frac{1}{\rho} \frac{\partial p}{\partial y} + \frac{1}{Re} \left(\frac{\partial^2 v}{\partial x^2} + \frac{\partial^2 v}{\partial y^2} \right)$$

Where, $u = (u, v)$ is a velocity vector, and p is pressure.

In the ANSYS FLUENT simulation, we employ the SIMPLE algorithm which stands for Semi Implicit Method for Pressure Linked Equations. [21] This is performed using a Pressure based solver which belongs to a general class of methods called the projection method. SIMPLE algorithm is a Pressure-based algorithm. This is different from the coupled algorithms such as SIMPLEC and PISO which we will not discuss in this report as these algorithms are not employed in the solving of the Navier Stokes equations of our particular case.

From a broader perspective, typical problem set up in FLUENT has the following steps [20]:

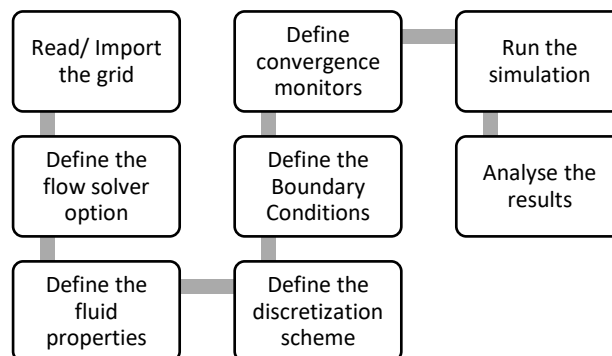


Figure 1. Steps in defining basic flows in Fluent [20]

PROBLEM SET-UP	SOLVER SET-UP
Define material properties	Use segregated solver like simple or coupled solver like SIMPLEC / PISO
Reynolds number, physical dimensions, flow velocity, viscosity	Choose the discretization type
Define boundary conditions	Choose grid type and cycle type
Provide initial conditions like $u = v = p = ?$	
Choose convergence monitors for averaged pressure and friction and slip / no-slip on the walls	

Figure 2. Solver and Problem set up for basic flows in ANSYS FLUENT [20]

In the segregated algorithm, the individual governing equations for the solution variables are solved one after another. This method of continuous iterations lies at the heart of CFD processing and it is what drives fluid flow simulations to convergence. The SIMPLE algorithm is memory efficient since the discretized equations need only be stored in the memory one at a time. The drawback being that the convergence is relatively slow. SIMPLEC/PISO algorithms do not need under relaxation and hence are faster in convergence than SIMPLE. According to the ANSYS theory guide, the steps involved in each iteration is given below in Figure 3.

As we will be dealing with incompressible flows in this project, so, density variation are not linked to the pressure and the mass conservation is a constraint on the velocity field; these equations (combined with the momentum) can be used to derive an equation for the pressure.

Solution of the steady-state NS equations is significant and in the SIMPLE algorithm, under-relaxation is used to increase stability (smoothing) where the variable under-relaxation is ϕ .

Where, $\phi = \phi_{old} + \alpha \Delta \phi$

and then implicit equation under-relaxation is given by,

$$\frac{\alpha_p \phi}{\alpha} = \sum \alpha_{nb} \phi_{nb} + b + \frac{1 - \alpha}{\alpha} \alpha_p \phi_{old}$$

Solution of the steady-state NS equations is of primary importance. For this, we shall define the equations as below:

Momentum equation,

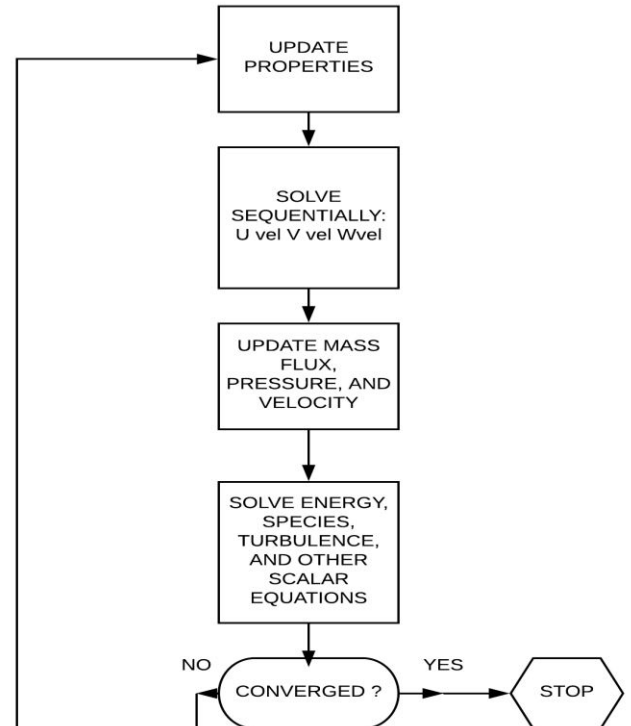


Figure 3 ANSYS Pressure based segregated solver flow diagram [19]

$$\frac{\partial u_i}{\partial t} + \frac{\partial u_j u_i}{\partial x_j} = \frac{\partial}{\partial x_j} \left(\mu \frac{\partial u_i}{\partial x_j} \right) - \frac{1}{\rho} \frac{\partial p}{\partial x_i}$$

Reference quantities,

$$\tilde{t} = \frac{t}{T} \quad \tilde{x}_i = \frac{x_i}{L} \quad \tilde{u}_i = \frac{u_i}{U} \quad \tilde{p} = \frac{p}{\rho U^2}$$

Non – dimensional equation,

$$St \frac{\partial u_i}{\partial t} + \frac{\partial u_j u_i}{\partial x_j} = \frac{1}{Re} \frac{\partial}{\partial x_j} \left(\mu \frac{\partial u_i}{\partial x_j} \right) - \frac{1}{\rho} \frac{\partial p}{\partial x_i}$$

Reynolds and Strouhal Number relations,

$$Re = \frac{UL}{\nu} \quad St = \frac{L}{TU} = \frac{fL}{U}$$

Computing an intermediate velocity field,

$$\alpha p(u_i)^* p = \sum_f \alpha_f (u_i^* \cdot n_i) f - \frac{1}{p} \frac{\partial p^n}{\partial x_i}$$

The equations are still non-linear; so, next we define a velocity and a pressure correction,

$$\left. \begin{aligned} u^{n+1} &= u^* + u' \\ p^{n+1} &= p^n + p' \end{aligned} \right\}$$

Using the definition and combining with an intermediate velocity field,

$$\alpha p(u_i)^{n+1} \cdot p = \sum_f \alpha_f (u_i^{n+1} \cdot n_i) f - \frac{1}{p} \frac{\partial p^{n+1}}{\partial x_i}$$

Deriving an equation for u' ,

$$\alpha p(u_i)' p = \sum_f \alpha_f [(u_i^{n+1} - u_i^*) \cdot n_i] f - \frac{1}{p} \frac{\partial p'}{\partial x_i}$$

Taking the divergence,

$$\frac{\partial}{\partial x_i} (u_i)^* p + \frac{\partial}{\partial x_i} (\tilde{u}_i)' - \frac{\partial}{\partial x_i} \left(\frac{1}{\alpha p} \frac{\partial p'}{\partial x_i} \right) = 0$$

We obtain a Poisson system for the pressure correction, solving it and computing a gradient,

$$(u_i)' p = (\tilde{u}_i)' - \frac{1}{\alpha p} \frac{\partial p'}{\partial x_i}$$

So, we can update

$$u^{n+1} = u^* + u'$$

Also, pressure at the next level,

$$p^{n+1} = p^n + p'$$

In the SIMPLE algorithm, under-relaxation is required due to the neglect of u^*

$$u^{n+1} = u^* + \alpha_u u' \text{ and } p = p^n + \alpha_p p'$$

There is an optimal relationship between α_u and α_p

$$\alpha_p = 1 - \alpha_u$$

SIMPLE Solution Algorithm [22]

In computational fluid dynamics (CFD), the SIMPLE algorithm is a widely used numerical procedure to solve the Navier-Stokes equations. Semi-Implicit Method for Pressure-Linked Equations (SIMPLE) family of algorithms is utilized for bringing pressure into the continuity equation. Due to the direct effect of pressure correction on velocity, this algorithm is defined as “Semi”. This algorithm damage a good velocity field unless we need to get a good pressure. Using this algorithm, the computation time might be minimized. For simple problems (e.g. laminar flow), convergence can be easily obtained. So, as stated before, the simple algorithm utilizes a connection between velocity and pressure corrections to satisfy mass conservation and get the pressure field [22].

Discretization: Fluent adopts a control-volume approach to change the governing equations to algebraic expressions that can be determined numerically. This control-volume method exists by integrating the governing equations about each control-volume. The governing equations can be illustrated more easily by assuming steady state conservation for transport of a scalar quantity ϕ .

Discretization scheme for convective terms in ANSYS [22]

1. First order upwind (Upwind Differencing)
2. Second order upwind (Total Variation Diminishing)
3. Third order upwind (QUICK), only for quad and hex

The written equation in integral form for an arbitrary control volume:

$$\int \rho \phi v \cdot dA = \int \Gamma_\phi \nabla_\phi \cdot dA + \int S_\phi dV \quad \text{---(1)}$$

Where,

$\rho = \text{density}$

$v = \text{velocity vector}$

$A = \text{Surface are vector}$

$\Gamma_\phi = \text{diffusion coefficient for } \phi$

$\nabla_\phi = \text{gradient of } \phi$

$S_\phi = \text{Source of } \phi \text{ per unit volume}$

Discretization of Equation (1) on a given cell gives:

$$\sum \rho_f \phi_f v_f \cdot A_f = \sum \Gamma_\phi (\nabla \phi)_n \cdot A_f + S_\phi V \quad \text{---(2)}$$

Where,

$\rho_f v_f A_f = \text{mass flux through face } f$

$A_f = \text{Area of the face}$

$(\nabla \phi)_n = \text{magnitude of } \nabla \phi \text{ normal to face } f$

$V = \text{Cell Volume}$

$\phi_f = \text{value of } \phi \text{ convected through face } f$

The equations solved by ANSYS FLUENT take the same general form as the one given above and apply readily to multi-dimensional, unstructured meshes composed of arbitrary polyhedral [22]. FLUENT stores discrete values of the scalar ϕ at the cell centers (c_0 & c_1). However, face values ϕ_f are required for the convection terms in equation (2) and must be interpolated from the cell center values.

The simple algorithm utilizes a connection between velocity and pressure corrections to satisfy mass conservation and get the pressure field. If we solved the momentum equation with an approximate pressure field p^* , the face flux, J_f^* , calculated from equation (1) will not satisfy the continuity equation.

$$J_f^* = \hat{J}_f d_f (p_{c_0}^* - p_{c_1}^*) \quad \text{---(4) where,}$$

$p_{c_0}^*$ and $p_{c_1}^* = \text{pressure within two cells on either side of the face}$

$\hat{J}_f = \text{Influence of velocities in the cell}$

$d_f = \text{average of momentum equation } a_p \text{ coefficients for the cell on either side of the face } f$

A correction factor J'_f must be added to the face flux J_f^* , so that the corrected face flux satisfies the continuity equation

$$J_f = J_f^* + J'_f \quad \text{---(5)}$$

The Simple algorithm suggests that J'_f can be expressed as:

$$J'_f = d_f (p'_{c_0} - p'_{c_1}) \text{ where } p' \text{ is cell pressure correction}$$

Substituting the flux correction equations (4) & (5), into the discrete continuity equation $\sum J_f A_f = 0$ yields to a discrete equation for the pressure correction p' in the cell

$$a_p p' = \sum a_{nb} p'_{nb} + b \quad \text{---(6)}$$

Where,

$b = \text{net flow into the cell}$

$$b = \sum J_f^* A_f$$

Then, the pressure correction equation (6) can be solved using the multigrid algebraic method [22]. When the solution is obtained, the cell pressure & face flux are corrected using the following equations:

$$p = p^* + \alpha_p p' \quad \text{---(7)}$$

$$J_f = J_f^* + d_f (p'_{c_0} - p'_{c_1}) \quad \text{---(8)}$$

Where,

α_p = under relaxation factor for pressure

Finally, the corrected face flux, J_f , satisfies the discrete continuity equation identically during each iteration

3. NUMERICAL RESULTS

1.1 *Lid driven cavity flow in two dimensions*: The fluid flow in a lid driven cavity is simulated by set of mass and momentum conservation equations. The flow is considered as two – dimensional, laminar, unsteady, incompressible and Newtonian. According to aforementioned conditions, below are the governing equations:

Continuity Equation: $\rightarrow \frac{\partial u}{\partial x} + \frac{\partial v}{\partial y} = 0$

x – Momentum Equation:

$$\rightarrow \frac{\partial u}{\partial t} + u \frac{\partial u}{\partial x} + v \frac{\partial u}{\partial y} = -\frac{1}{\rho} \frac{\partial p}{\partial x} + \frac{1}{Re} \left(\frac{\partial^2 u}{\partial x^2} + \frac{\partial^2 u}{\partial y^2} \right)$$

y – Momentum equation:

$$\begin{aligned} \rightarrow \frac{\partial v}{\partial t} + u \frac{\partial v}{\partial x} + v \frac{\partial v}{\partial y} &= -\frac{1}{\rho} \frac{\partial p}{\partial y} + \frac{\mu}{\rho} \left(\frac{\partial^2 v}{\partial x^2} + \frac{\partial^2 v}{\partial y^2} \right) \\ \rightarrow \frac{\partial v}{\partial t} + u \frac{\partial v}{\partial x} + v \frac{\partial v}{\partial y} &= -\frac{1}{\rho} \frac{\partial p}{\partial y} + \frac{1}{Re} \left(\frac{\partial^2 v}{\partial x^2} + \frac{\partial^2 v}{\partial y^2} \right) \end{aligned}$$

“ u ” and “ v ” are velocity in “ x ” and “ y ” direction, “ t ” is time, “ ρ ” is density and “ μ ” is dynamic viscosity. The vorticity transport equation can be obtained by compiling stream function and vorticity equation. The equations are:

$$\begin{aligned} \rightarrow \frac{\partial \Omega}{\partial t} + u \frac{\partial \Omega}{\partial x} + v \frac{\partial \Omega}{\partial y} &= \frac{1}{Re} \left(\frac{\partial^2 \Omega}{\partial x^2} + \frac{\partial^2 \Omega}{\partial y^2} \right) \\ \rightarrow \frac{\partial^2 \psi}{\partial x^2} + \frac{\partial^2 \psi}{\partial y^2} &= 0 \end{aligned}$$

Dimensions of the square cavity and the lid velocity are set to unity as mentioned in publication by “Alejandro Allievi and Rodolfo Bermejo” then Reynolds Number is inversely proportional to kinematic viscosity. The case is unsteady and the fluid is incompressible. Calculations are performed using Mesh [62 x40] with Quads face mesh in a 2D Model as shown below:

Mesh	Nodes	Mesh Matrix (Element Quality)			
		Min	Max	Average	Std. Deviation
62 X 40	2646	0.90927	0.99853	0.91757	2.2572e-002

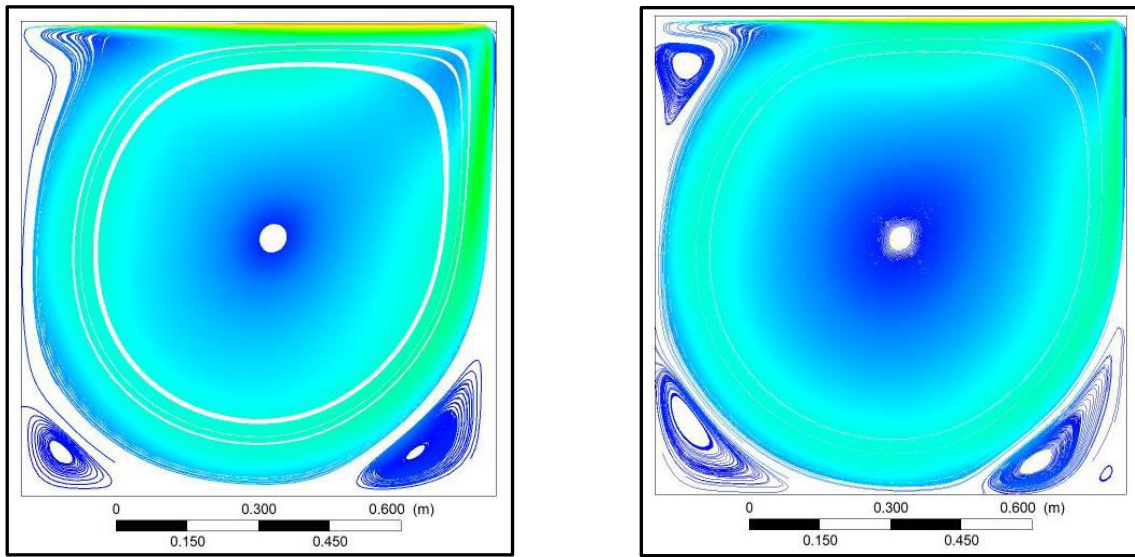


Figure 4: Streamlines, Re 3200 and Re 10000, Mesh 62 X 40

All the simulations are carried out up to number of iterations where convergence criteria of 10^{-3} was met. Flow time in lid driven cavity was 150 sec. The Lid was given initial velocity of 0m/sec and after certain time the lid was moving with the constant velocity of 1 m/sec. Reynolds number used in these computations are 3200 and 10000. Going towards higher Reynolds number increases the number of iterations to get to required convergence criteria. These two values of Reynolds number coincide with those identified in the experimental computation of Alejandra and Rodolfo as the range where parts of the flow appeared to change from laminar to turbulent. In Re3200 computation, continuity solution is converged up to $6.6786e-04$, for x – velocity $3.9982e-07$ and for y – velocity $3.0543e-07$ and in Re10000, continuity solution converged up to $8.9301e-04$, for x – velocity $1.4771e-07$ and for y – velocity $1.0943e-07$.

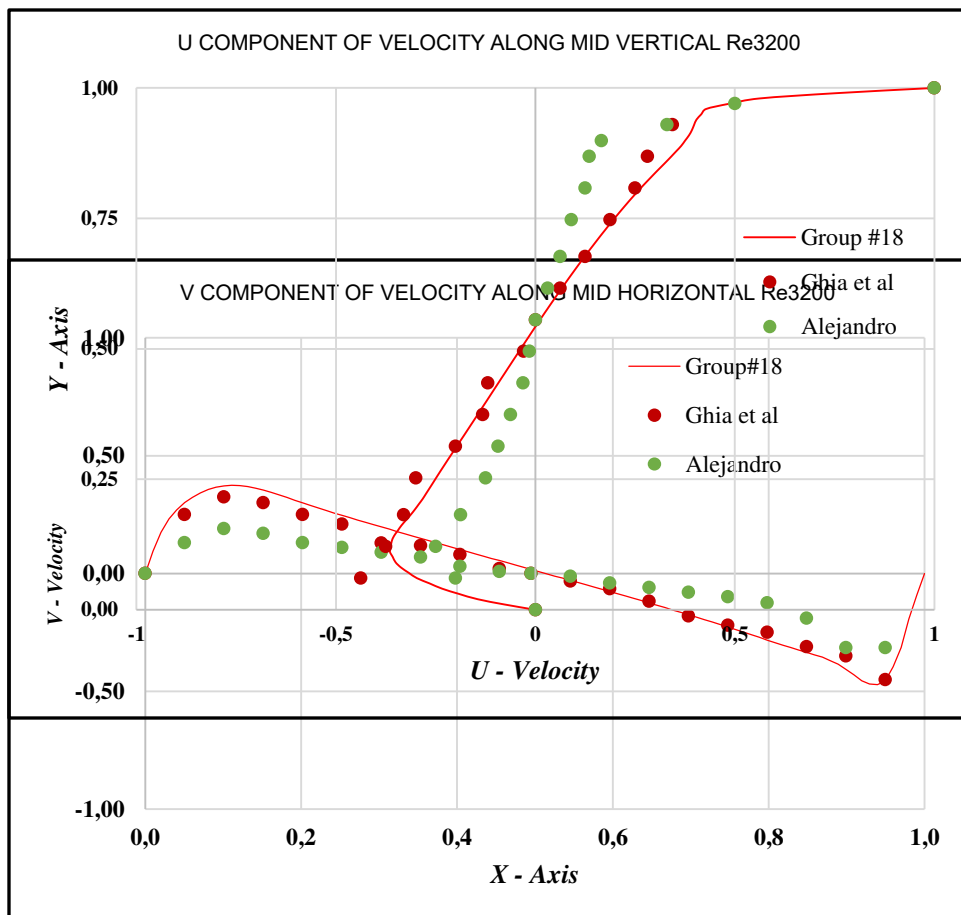


Figure 5: Cavity Flow. Re 3200. Velocity profiles at mid horizontal and vertical lines.

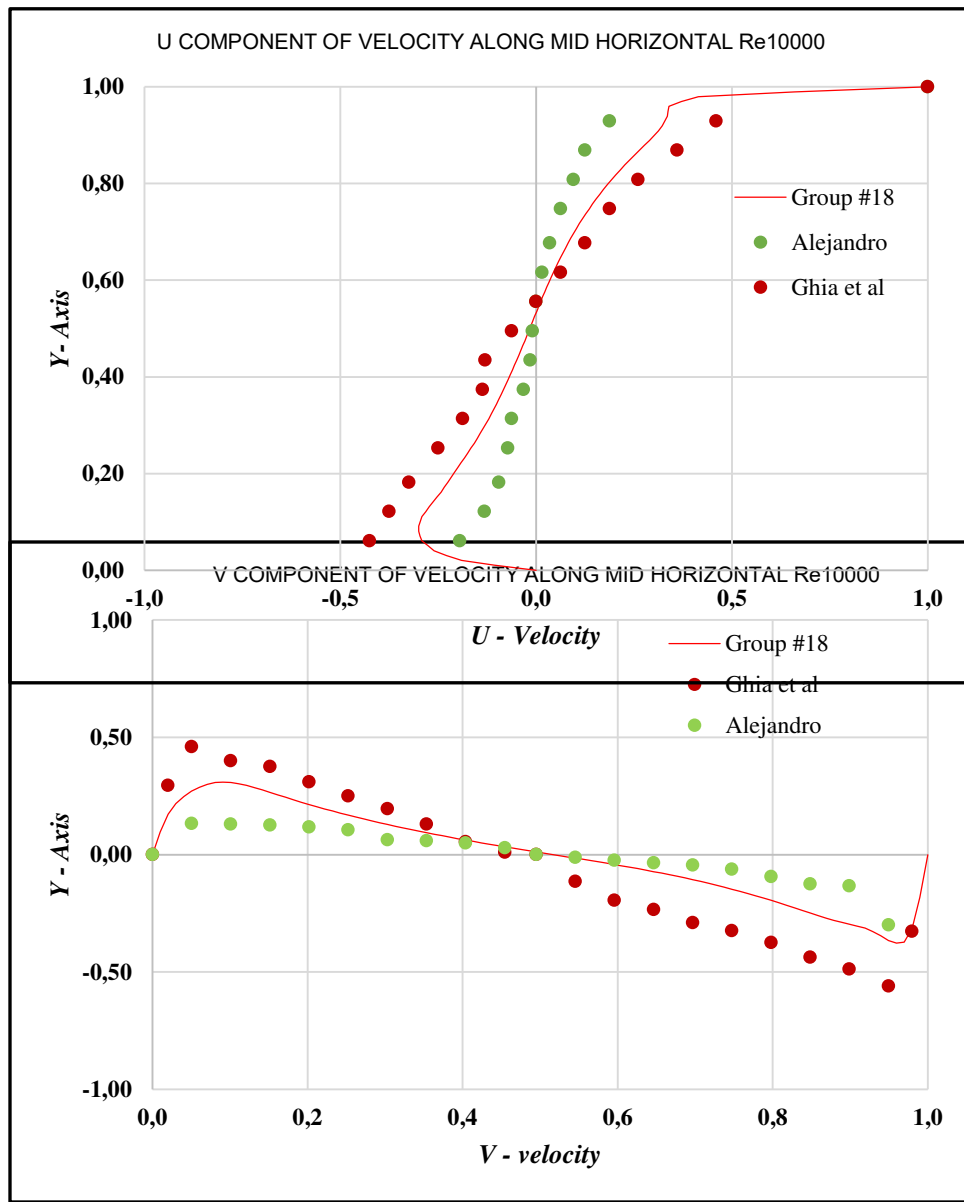


Figure 6: Cavity Flow. Re 10000. Velocity profiles at mid horizontal and vertical lines.

Figure 5 and Figure 6 show the u and v -velocity profiles along a vertical and horizontal line respectively passing through the geometric center of the square cavity for $AR=1$ (Aspect Ratio = Height/Length). As can be seen there is favorable agreement in the velocity profile between CFD simulations in this study and the respected compared data. Cavity flow with $Re\ 3200$ exhibits a large primary vortex with two secondary vortices in the two bottom corners whereas, Flow with $Re10000$ has three secondary vortices with large primary vortex at the center. Simulations of 2D lid driven cavity flow has already been performed for wide range of Reynolds number by various authors. Simulation results for incompressible laminar flow in square cavity are compared to data of Alejandro and Ghia et al and are also presented above, to verify the validity of the CFD simulation solution. The method used by Alejandro to produce results was Finite Element Method of Modified Characteristics with quadratic elements and quad elements are used in this study to reproduce the results by using pressure based solver in ANSYS.

1.2 Flow around a circular cylinder at $Re=100$: The computational domain and the boundary conditions for the simulation of the flow around circular cylinder are shown in Figure 4. The circular cylinder is simulated with the characteristic length scale of 20 m in the direction perpendicular to the streamflow. The center of cylinders is located at origin of the coordinate system. Longitudinal uniform velocities varying from 0 to 1 m/s were introduced at the inlet of the channel, corresponding to $Re\ 100$.

Relatively fine mesh has been created using triangle mesh with a maximum face size of 0.30m and edge sizing of circular cylinder is done with element size of 0.25m. To monitor the flow over circular region we have inflated the regions into 40 layers with first layer thickness of 0.25m with a growth rate of 2.5. Uniform flow was assumed at the entrance of the channel. Walls of the channel are put to stationary condition and flow is directed towards the circular cylinder. The flow simulations was carried out with 3000 times step with a step size of 0.1 and 20 iterations with each step making the fluid to flow over cylinder for 300 sec.

Along with this mesh, another mesh with quadratic elements has been generated close to mesh used by Rodolfo and Alejandro in their publication. Results of these two meshes using pressure based solver and FEMMC results of Alejandro are compared.

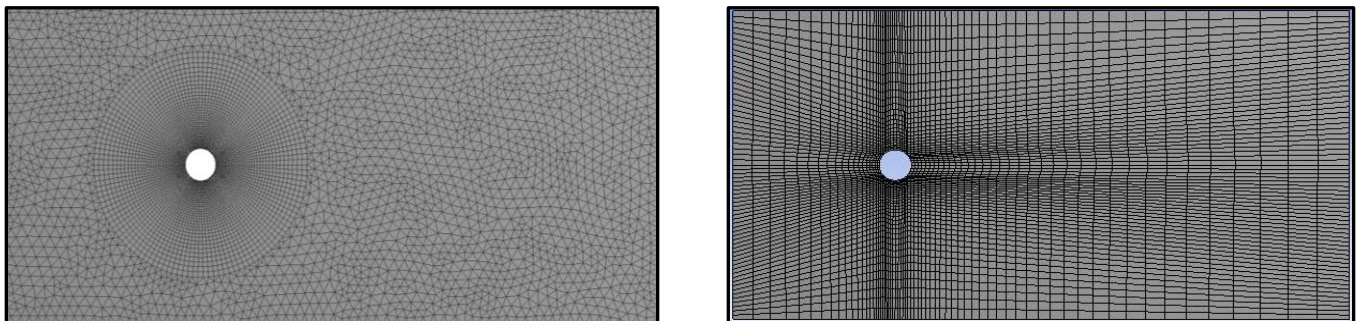


Figure 7. Flow around Circular Cylinder Re100. Finite Element Mesh

The results of the flow are shown below from $t = 10$ sec to 120 sec. No initial provoking was done to begin the asymmetry in the wake. The vortex shredding starts at 24 sec and becomes asymmetric at approximately 17 sec. When the boundary layer separates, they create a shear layer. They develop waves that roll up into vortices. We can observe that there are two shear layers behind the circular cylinder. On the outside the flow goes forward and backwards on the inside. They shed alternatively

from each side of the cylinder. The vortex shredding frequency “ f ” is the function of flow velocity and the distance between the shear layers.

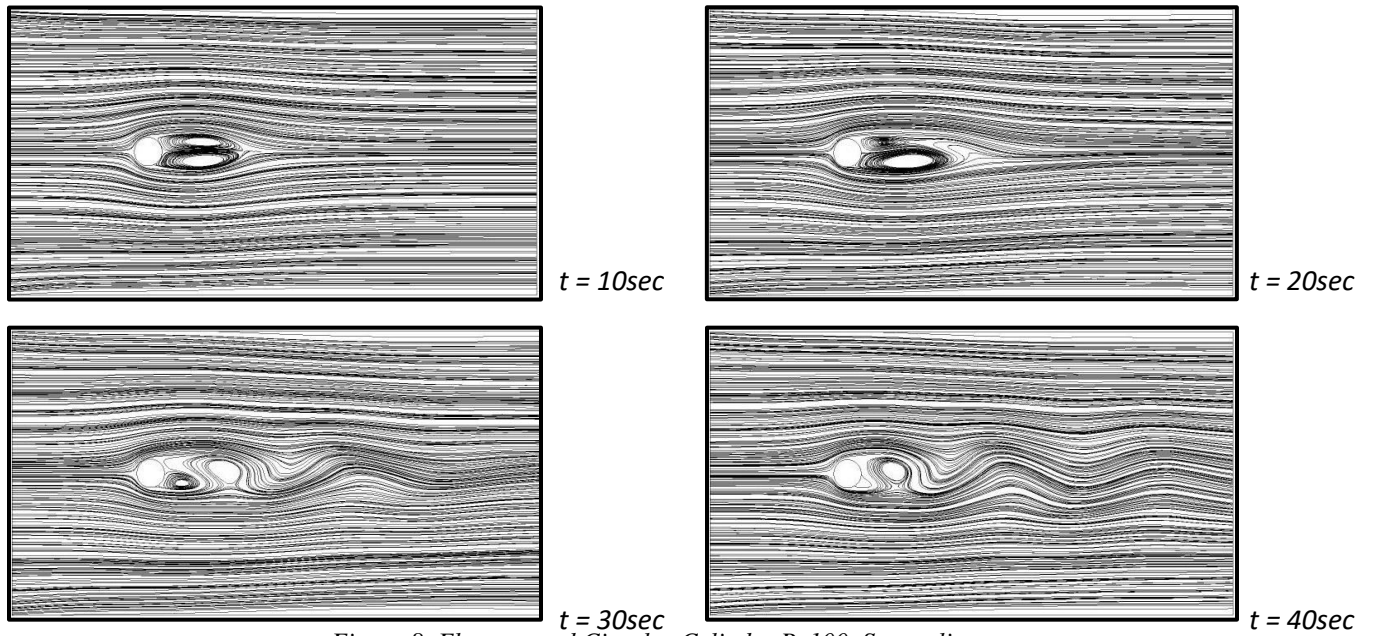
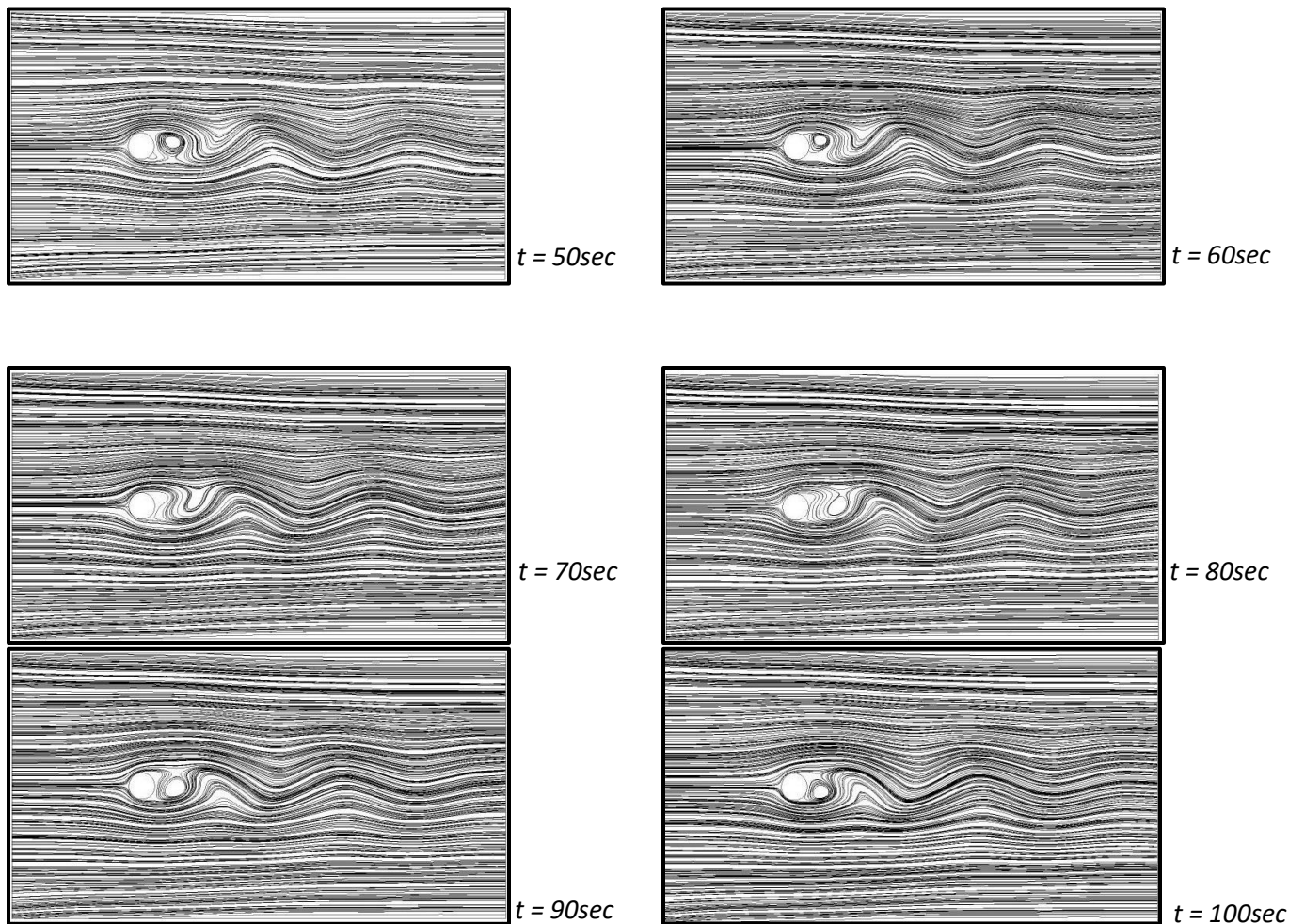


Figure 8. Flow around Circular Cylinder $Re=100$. Streamlines



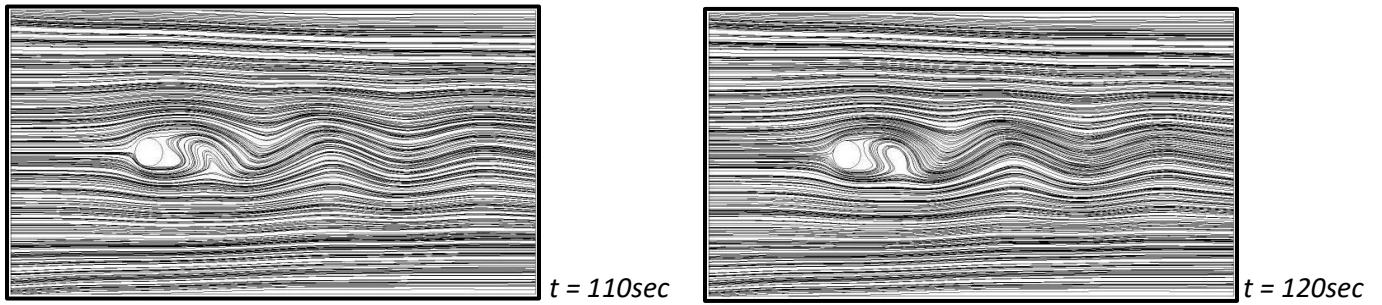


Figure 6. Flow around Circular Cylinder $Re100$. Streamlines

A periodical motion with uniform amplitude is obtained at 70 sec. The period of oscillation for section, around 75 to 85 sec is 5.3 sec and these results in Strouhal Number of 0.188. Below is the table for comparison of results with experimental and numerical data compiled by “Alejandro and Ghia et al.”.

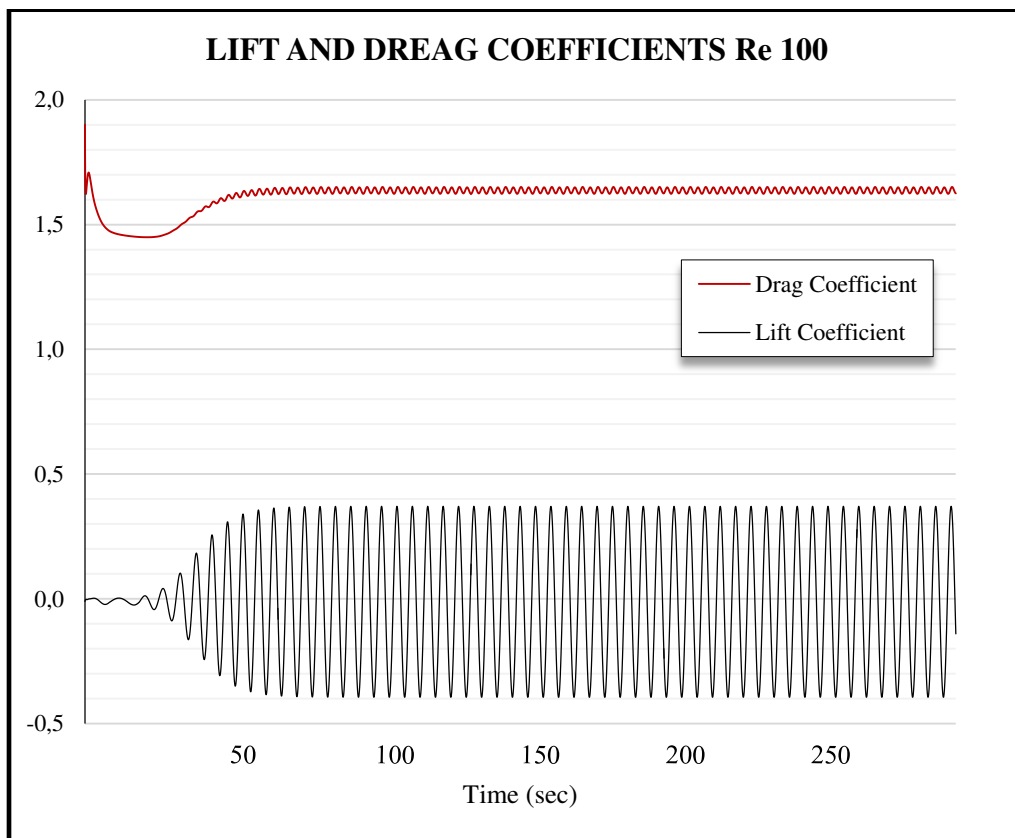


Figure 7. Flow around Circular Cylinder $Re100$. Force Coefficients.

Table 1: Comparison of Results

Flow around circular cylinder at $Re = 100$			
Ghia et al	Alejandro & Rodolfo	This Work	
		Triangle Mesh	Quad Mesh

Strouhal Number	0.16	0.167	0.192	0.188
Mean Drag coefficient	1.25-1.46	1.295	1.664	1.625
RMS of fluctuating Drag coefficient	0.0042-0.04	0.0085	0.025	0.012
RMS of fluctuating Lift coefficient	0.157-0.39	0.162	0.264	0.249

4. CONCLUSION

The lid-driven cavity problem has been studied for two different Reynolds numbers. It was designed to improve the calculation of viscous forces acting on the particles in the vicinity of the walls. Close agreement with reference data has been obtained, hence demonstrating the potential capabilities and competitiveness of the pressure based algorithm. Flow field and variation in the drag coefficient of two-dimensional flow past vertical cylinders were analyzed using ANSYS Pressure based solver and SIMPLE model. Vortex shedding and the wake flow developed behind the cylinders were significantly influenced by cylinder shape. It can also be observed, that slightly different result is obtained by triangular mesh as that of the quad mesh. The accuracy of computational analysis could be improved further by meshing with higher density the entire domain of analysis. The flow around cylinder is still a subject of research because in the complex processes of flow still is not imposed only one method or solution of determination the specific unknowns. Being the simplest possible closed shape, at this point are meeting in a large enough way the analytical theories and experiments.

REFERENCES

1. Zhiyong Si, “Second order modified method of characteristics mixed defect-correction finite element method for time dependent Navier–Stokes problems”, (2011)
2. Girault, V., Raviart, P.A., “Finite Element Method for Navier–Stokes Equations: Theory and Algorithms”, (1987)
3. Hansbo, P., “The characteristic streamline diffusion method for the time-dependent incompressible Navier–Stokes equations”, (1992)
4. He, Y.N., Sun, W.W., “Stability and convergence of the Crank-Nicolson/Adams-Bashforth scheme for the time-dependent Navier–Stokes equations”, (2007)
5. He, Y.N., Li, J., “Convergence of three iterative methods based on the finite element discretization for the stationary Navier–Stokes equations”, (2009)
6. J.P. Benque, B. Iblier, A. Keramsi and G. Labadie, “A finite element method for Navier–Stokes equations coupled with a temperature equation”, (1982)
7. J. Douglas and T.F. Russell, “Numerical methods for convection-dominated diffusion problems based on combining the method of characteristics with finite element or finite difference procedures”, (1982)
8. O. Pironneau, “On the transport-diffusion algorithm and its applications to the Navier–Stokes equations”, (1982)
9. Dawson, C.N., Russell, T.F., Wheeler, M.F., “Some improved error estimates for the modified method of characteristics”, (1989)
10. Buscaglia, G., Dari, E.A., “Implementation of the Lagrange–Galerkin method for the incompressible for the incompressible Navier–Stokes equations”, (1992)
11. A. Allievi and R. Bermejo, “A generalized particle search–locate algorithm for arbitrary grids”, (1997)
12. A. Allievi and R. Bermejo, “Finite element modified method of characteristics for the Navier-Stokes equations”, (2000)
13. J. Cahouet and J.P. Chabard, “Some fast 3D finite element solvers for the generalized Stokes problem”, (1988)
14. E.J. Dean and R. Glowinski, “On some finite element methods for the numerical simulation of incompressible viscous flow”, (1993)
15. M.O. Bristeau, R. Glowinski and J. Periaux, “Numerical methods for the Navier–Stokes equations. Applications to the simulation of compressible and incompressible viscous flows”, (1987)
16. U. Ghia, K.N. Ghia and C.T. Shin, “High-Re solutions for the incompressible flow using the Navier–Stokes equations and a multigrid method”, (1982)
17. Schäfer M., Turek S., Durst F., Krause E., Rannacher R., “Benchmark Computations of Laminar Flow Around a Cylinder”, (1996)
18. <https://summerofhpc.prace-ri.eu/magic-behind-the-most-of-the-cfd-solvers-for-hpc/>

19. *FLUENT User Guide, Section 9.2 Continuity and Momentum Equations*
20. *Stanford University Lecture notes ME469B*
<https://www.google.com/url?q=https://web.stanford.edu/class/me469b/handouts/incompressible.pdf&sa=D&ust=1542429161913000&usg=AFQjCNG2D3MX8bHOzAUiG9W9CXXlHP1qsg>
21. *FLUENT User Guide, Section 25.1.1 Pressure Based Solver*
22. *FLUENT User Guide, Chapter 22 SIMPLE Solution Method* , <http://www.afs.enea.it/fluent/>